

Construction of control barrier function and C^2 reference trajectory for constrained attitude maneuvers

Xiao Tan and Dimos V. Dimarogonas

Division of Decision and Control Systems
School of Electrical Engineering and Computer Science
KTH Royal Institute of Technology, Sweden

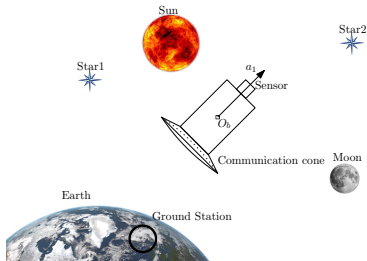
IEEE-CDC 2020



Swedish
Research
Council

Motivation

Constrained attitude maneuvers

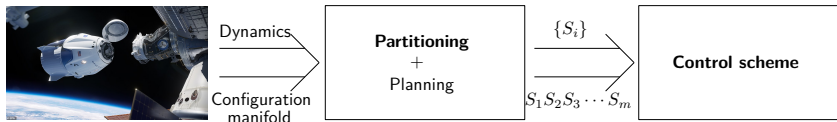


Spacecraft maneuvering while avoiding bright objects and always maintaining communication

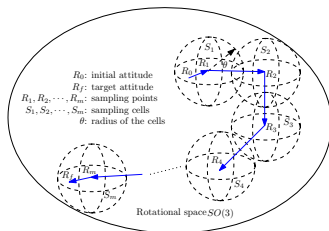


Spacecraft docking with ISS
credit: NASA TV

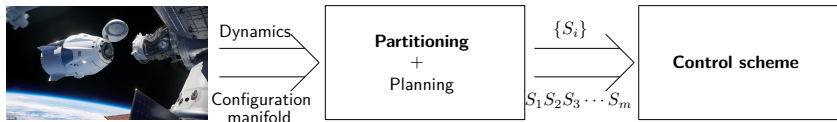
Solution Overview



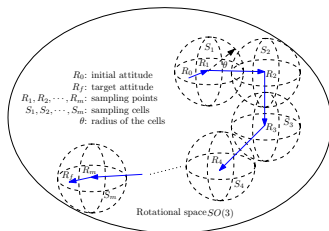
C^2 reference curve construction



Solution Overview



C^2 reference curve construction
High-order CBF construction



Problem illustration

- attitude dynamics

$$\begin{cases} \dot{R} = R[\omega]_{\times}, \\ J\dot{\omega} + [\omega]_{\times}J\omega = u, \end{cases} \quad \text{with } [\omega]_{\times} := \begin{pmatrix} 0 & -\omega_3 & \omega_2 \\ \omega_3 & 0 & -\omega_1 \\ -\omega_2 & \omega_1 & 0 \end{pmatrix}. \quad (1)$$

¹Xiao Tan, Soulaïmane Berkane, and Dimos V. Dimarogonas. Constrained attitude maneuvers on $SO(3)$: Rotation space sampling, planning and low-level control. *Automatica*, 112, 2020.

Problem illustration

- attitude dynamics

$$\begin{cases} \dot{R} = R[\omega]_{\times}, \\ J\dot{\omega} + [\omega]_{\times}J\omega = u, \end{cases} \quad \text{with } [\omega]_{\times} := \begin{pmatrix} 0 & -\omega_3 & \omega_2 \\ \omega_3 & 0 & -\omega_1 \\ -\omega_2 & \omega_1 & 0 \end{pmatrix}. \quad (1)$$

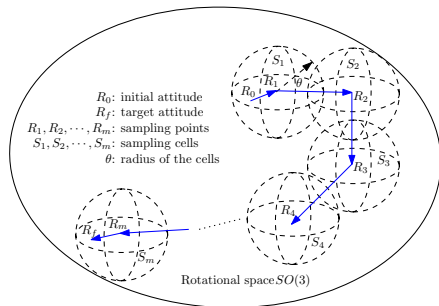
Sampling set

$$U := \{R_1, R_2, \dots, R_i, \dots, R_n\}.$$

Index set $\mathcal{N} = \{1, 2, \dots, n\}$.

Cell region $S_i := \{R \in SO(3) : d(R, R_i) < \theta, i \in \mathcal{N}\}$, $\theta \in (0, \pi/2)$.

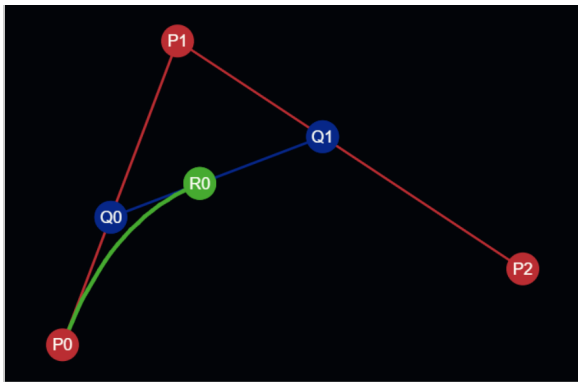
The neighborhood set N_i of R_i
 $N_i := \{R \in U : d(R, R_i) < 2\theta, R \neq R_j, i \in \mathcal{N}\}$.



¹Xiao Tan, Soulaïmane Berkane, and Dimos V. Dimarogonas. Constrained attitude maneuvers on $SO(3)$: Rotation space sampling, planning and low-level control. *Automatica*, 112, 2020.

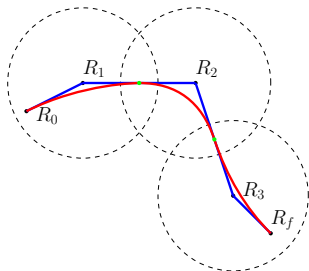
Reference generation: Bézier curve

Bézier curve: **recursive linear interpolation**



<http://www.malinc.se/m/DeCasteljauAndBezier.php>

Reference generation: Bézier curve

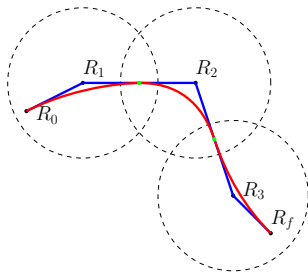


A concatenated Bézier curve $c : [0, m] \rightarrow SO(3)$ is defined as

$$c(\tau) = \begin{cases} c_{R_0, R_1, R_{1,2}}(\tau) & \tau \in [0, 1), \\ c_{R_{i-1, i}, R_i, R_{i, i+1}}(\tau - i + 1) & \tau \in [i - 1, i), \\ & i \in \{2, 3, \dots, m - 1\}, \\ c_{R_{m-1, m}, R_m, R_f}(\tau - m + 1) & \tau \in [m - 1, m], \end{cases}$$

where $R_{i, i+1} := R_i \exp(1/2 \log(R_i^\top R_{i+1}))$.

Reference generation: Bézier curve

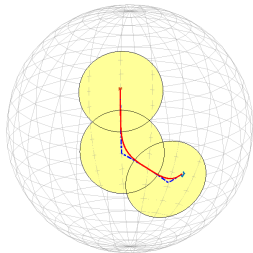
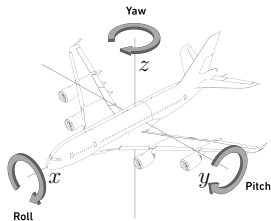


The Bézier curve has the following properties:

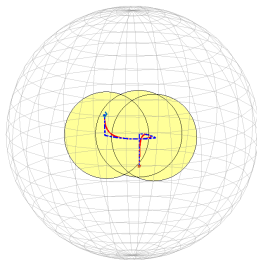
- $c(0) = R_0, c(m) = R_f$;
- $c(\tau) \in \cup_{i=1}^m S_i$ for $\tau \in [0, m]$;
- $c(\tau)$ is a C^2 curve;

*To obtain the reference trajectory (parametrized with time t), we need re-parametrize the paths with $\tau(t) : [0, T_f] \rightarrow [0, m]$, which is neglected here.

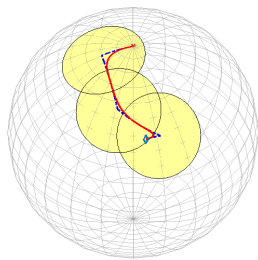
Simulation: Geodesic path v.s. Bézier curve



Trajectory of x-axis.



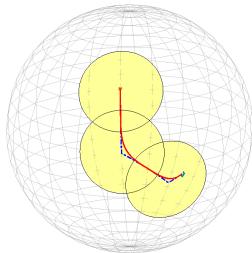
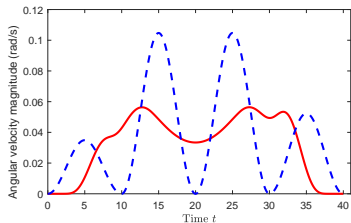
Trajectory of y-axis.



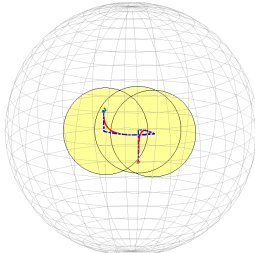
Trajectory of z-axis.

Blue: geodesic path; Red : Bézier curve.

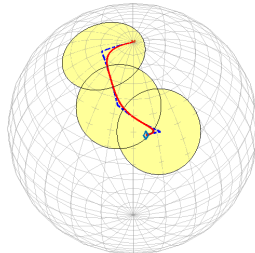
Simulation: Geodesic path v.s. Bézier curve



Trajectory of x-axis.



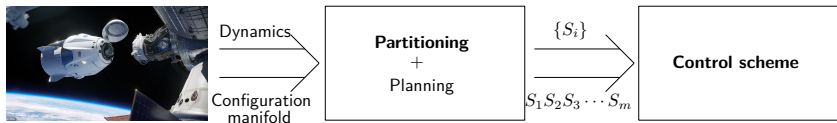
Trajectory of y-axis.



Trajectory of z-axis.

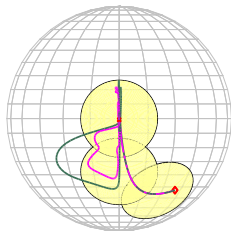
Blue: geodesic path; Red : Bézier curve.

Overview



High-order CBF construction

- Non-smoothness
- Possible singularities



Control barrier function design

Define $r_i : SO(3) \rightarrow \mathbb{R}$

$$r_i(R) = \epsilon - \|R_i - R\|_F^2/2. \quad (2)$$

with $\epsilon := 4 \sin^2(\theta/2)$.

- $r_i(R) > 0$ iff $R \in S_i$.

²P. Glotfelter, J. Cortes, and M. Egerstedt, Nonsmooth barrier functions with applications to multi-robot systems, IEEE control systems letters, 2017.

Control barrier function design

Define $r_i : SO(3) \rightarrow \mathbb{R}$

$$r_i(R) = \epsilon - \|R_i - R\|_F^2/2. \quad (2)$$

with $\epsilon := 4 \sin^2(\theta/2)$.

- $r_i(R) > 0$ iff $R \in S_i$.
-

$$R(t) \in \cup_{i \in \mathcal{N}} S_i \iff \max_{i \in \mathcal{N}}(r_i(R(t))) > 0, \quad \text{for } t \geq 0. \quad (3)$$

max operation \Rightarrow nonsmooth analysis and a complex formulation[2].

²P. Glotfelter, J. Cortes, and M. Egerstedt, Nonsmooth barrier functions with applications to multi-robot systems, IEEE control systems letters, 2017.

CBF design: Non-smoothness

- Define

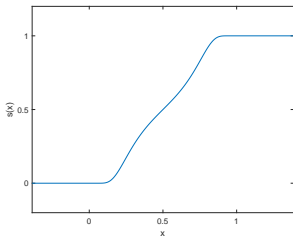
$$h(R) = \sum_{i \in \mathcal{N}} s(r_i(R)/\epsilon) - \delta, \quad (4)$$

where constant $\delta > 0$.

Here

$$s(x) = \begin{cases} 0 & x \in (-\infty, 0] \\ \frac{\rho(x)}{\rho(x) + \rho(1-x)} & x \in (0, 1), \\ 1 & x \in [1, \infty) \end{cases}$$

with $\rho(x) := (1/x)e^{-1/x}$.



CBF design: Non-smoothness

- Define

$$h(R) = \sum_{i \in \mathcal{N}} s(r_i(R)/\epsilon) - \delta, \quad (4)$$

where constant $\delta > 0$.

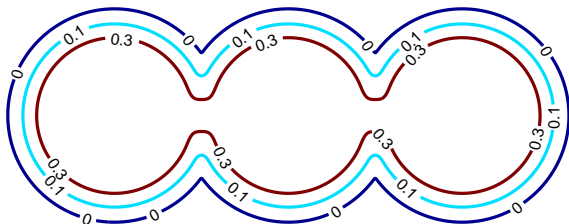


Illustration of C_h in the planar case with different conservativeness δ' s.

CBF design: High-order systems

To comply with the control affine form, rewriting the attitude dynamics, we have

$$\dot{x} := f(x) + gu,$$

$$\text{where } x = \begin{pmatrix} r_{11} \\ r_{12} \\ \dots \\ r_{33} \\ \omega_1 \\ \omega_2 \\ \omega_3 \end{pmatrix} \in \mathbb{R}^{12}, f(x) = \begin{pmatrix} r_{12}\omega_3 - r_{13}\omega_2 \\ r_{13}\omega_1 - r_{11}\omega_3 \\ r_{11}\omega_2 - r_{12}\omega_1 \\ r_{22}\omega_3 - r_{23}\omega_2 \\ r_{23}\omega_1 - r_{21}\omega_3 \\ r_{21}\omega_2 - r_{22}\omega_1 \\ r_{32}\omega_3 - r_{33}\omega_2 \\ r_{33}\omega_1 - r_{31}\omega_3 \\ r_{31}\omega_2 - r_{32}\omega_1 \\ J^{-1}(-[\omega]_{\times} J\omega) \end{pmatrix}, g = \begin{pmatrix} 0_{9 \times 3} \\ J^{-1} \end{pmatrix}.$$

CBF design: High-order systems

To comply with the control affine form, rewriting the attitude dynamics, we have

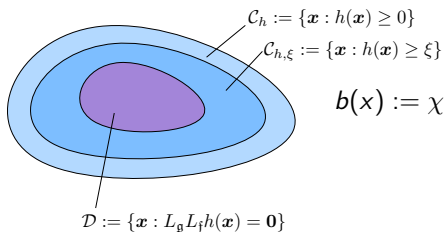
$$\dot{x} := f(x) + gu,$$

$$\text{where } x = \begin{pmatrix} r_{11} \\ r_{12} \\ \dots \\ r_{33} \\ \omega_1 \\ \omega_2 \\ \omega_3 \end{pmatrix} \in \mathbb{R}^{12}, f(x) = \begin{pmatrix} r_{12}\omega_3 - r_{13}\omega_2 \\ r_{13}\omega_1 - r_{11}\omega_3 \\ r_{11}\omega_2 - r_{12}\omega_1 \\ r_{22}\omega_3 - r_{23}\omega_2 \\ r_{23}\omega_1 - r_{21}\omega_3 \\ r_{21}\omega_2 - r_{22}\omega_1 \\ r_{32}\omega_3 - r_{33}\omega_2 \\ r_{33}\omega_1 - r_{31}\omega_3 \\ r_{31}\omega_2 - r_{32}\omega_1 \\ J^{-1}(-[\omega]_{\times} J\omega) \end{pmatrix}, g = \begin{pmatrix} 0_{9 \times 3} \\ J^{-1} \end{pmatrix}.$$

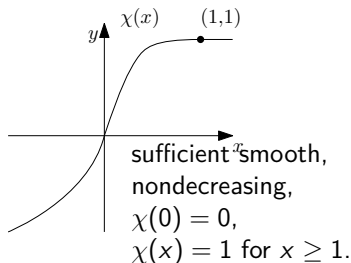
$L_g h(x) = 0$ for all x . **Cannot apply ZBF directly.**

CBF design: Intuitions behind singularity-free HOCBF

Prop.3: $\mathcal{D} \subset \mathcal{C}_{h,\xi}$.

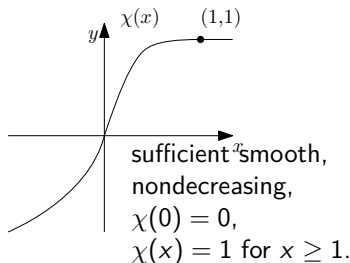
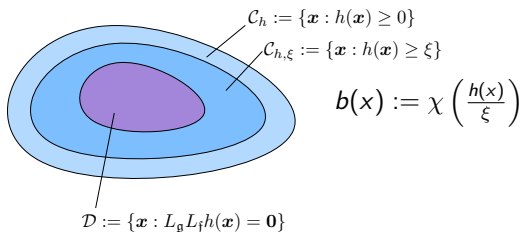


$$b(x) := \chi\left(\frac{h(x)}{\xi}\right)$$



CBF design: Intuitions behind singularity-free HOCBF

Prop.3: $\mathcal{D} \subset \mathcal{C}_{h,\xi}$.



- $\mathcal{C}_b = \mathcal{C}_h$.
- For $x \in \mathcal{C}_{h,\xi}$, we derive that, for $1 \leq k \leq r$,

$$b(x) = 1 > 0$$

$$b_1(x) := \dot{b}(x) + \alpha(b(x)) = \alpha(1) > 0$$

$$L_g L_f b(x)u + L_f b_1(x) + \beta(b_1(x)) = \beta \circ \alpha(1) > 0$$

Thus, b is a high-order CBF.

Singularity-free HOCBF

Concretely, the modified controller is given by

$$\begin{aligned} u(x) &= \arg \min_{u \in \mathbb{R}^3} \|u - u_{nom}\|^2 \\ \text{s.t. } & L_g L_f b(x)u + L_f b_1(x) + \beta(b_1(x)) \geq 0. \end{aligned} \tag{5}$$

Singularity-free HOCBF

Concretely, the modified controller is given by

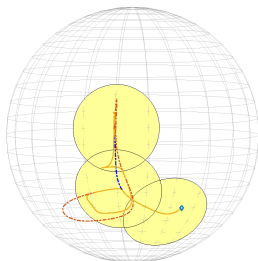
$$\begin{aligned} u(x) &= \arg \min_{u \in \mathbb{R}^3} \|u - u_{nom}\|^2 \\ \text{s.t. } & L_g L_f b(x)u + L_f b_1(x) + \beta(b_1(x)) \geq 0. \end{aligned} \tag{5}$$

Theorem

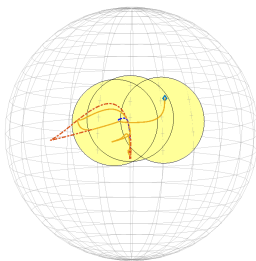
For the attitude control system in (1), the controller (5) renders the set $\mathcal{C}_b \cap \mathcal{C}_{b_1}$ forward invariant.

Simulation: Reference tracking controller

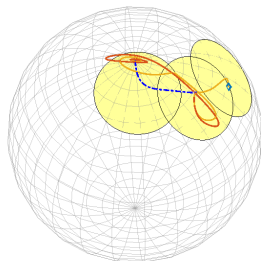
An additive control signal $u_{add}(t)$ for $t \in [20, 25]$ is used in **Red** and **Orange** Cases to imitate human inputs to the system.



Trajectory of x-axis.



Trajectory of y-axis.



Trajectory of z-axis.

Blue: Reference tracking control with no additive signal; control barrier function exists;

Red: Reference tracking control with additive signal; control barrier function does not exist;

Orange: Reference tracking control with additive signal; control barrier function exists.

Conclusion

In the talk, we present

- a **Bézier curve-based** reference trajectory for cell transitions in $SO(3)$, and,

Conclusion

In the talk, we present

- a **Bézier curve-based** reference trajectory for cell transitions in $SO(3)$, and,
- a **high-order barrier function** that ensures the transient performance for cell transitions.

Latest work

High-order control barriers:

- forward invariance and asymptotic stability of the set \mathcal{C} ;
- singularity-free, performance-critical design.

Xiao Tan, Wenceslao Shaw-Cortez, and Dimos V. Dimarogonas.
High-order barrier functions: robustness, safety and performance-critical control. *IEEE Transactions of Automatic Control*, under review.

Thank you for your attention!

